A Random-Sequential Mechanism for Nitrite Binding and Active Site Reduction in Copper-containing Nitrite Reductase

Wijma, H.J.; Jeuken, L.J.C.; Verbeet, M.P.; Armstrong, F.A.; Canters, G.W.

THE JOURNAL OF BIOLOGICAL CHEMISTRY VOL. 281, NO. 24, pp. 16340–16346, June 16, 2006

A Random-sequential Mechanism for Nitrite Binding and Active Site Reduction in Copper-containing Nitrite Reductase*[S]

Received for publication, February 21, 2006, and in revised form, April 12, 2006 Published, JBC Papers in Press, April 13, 2006, DOI 10.1074/jbc.M601610200

Hein J. Wijma[‡1], **Lars J. C. Jeuken**[§], **Martin P. Verbeet**[‡], **Fraser A. Armstrong**[¶], **and Gerard W. Canters**[‡2]

From the [‡]*Leiden Institute of Chemistry, Leiden University, P.O. Box 9502, 2300 RA Leiden, The Netherlands, the* [§]*Institute of Molecular Biophysics, University of Leeds, Leeds LS2 9JT, United Kingdom, and the* [¶]*Inorganic Chemistry Laboratory, Oxford University, South Parks Road, Oxford OX1 3QR, United Kingdom*

The homotrimeric copper-containing nitrite reductase (NiR) contains one type-1 and one type-2 copper center per monomer. Electrons enter through the type-1 site and are shuttled to the type-2 site where nitrite is reduced to nitric oxide. To investigate the catalytic mechanism of NiR the effects of pH and nitrite on the turnover rate in the presence of three different electron donors at saturating concentrations were measured. The activity of NiR was also measured electrochemically by exploiting *direct* electron transfer to the enzyme immobilized on a graphite rotating disk electrode. In all cases, the steady-state kinetics fitted excellently to a random-sequential mechanism in which electron transfer from the type-1 to the type-2 site is rate-limiting. At low [NO_2^-] reduction of the type-2 site precedes nitrite binding, at high [NO_2^-] the reverse occurs. Below pH 6.5, the catalytic activity diminished at higher nitrite concentrations, in agreement with electron transfer being slower to the nitrite-bound type-2 site than to the water-bound type-2 site. Above pH 6.5, substrate activation is observed, in agreement with electron transfer to the nitrite-bound type-2 site being faster than electron transfer to the hydroxyl-bound type-2 site. To study the effect of slower electron transfer between the type-1 and type-2 site, NiR M150T was used. It has a type-1 site with a 125-mV higher midpoint potential and a 0.3-eV higher reorganization energy leading to an ~50-fold slower intramolecular electron transfer to the type-2 site. The results confirm that NiR employs a random-sequential mechanism.

Copper-containing nitrite reductase (NiR)[3] is one of the enzymes of the denitrification pathway (1). Denitrification globally recycles fixed nitrogen (NO_3^-, NO_2^-) to the atmosphere (N_2) with NO and N_2O being formed as by-products; they act as ozone scavenger and as greenhouse gas, respectively (2, 3). Copper-containing nitrite reductases are found in bacteria, Archaea, and fungi (1, 4, 5). In pathogens, copper-containing NiR is known to enhance the resistance against human sera in *Neisseria gonorrhoeae* (6) and allows *Neisseria meningitidis* to respire on nitrite under the microaerobic conditions encountered during disease in humans (7). Furthermore, there is an interest in applying NiR in amperometric biosensors for selectively monitoring toxic nitrite in natural waters and waste streams (8–10).

NiR is a homotrimer, in which each subunit contains a type-1 copper site that accepts electrons from a physiological electron donor and transfers them to a type-2 copper site that is located deeper inside the enzyme (11–13). The type-2 copper is coordinated by three histidines and forms the active site together with a water network, an aspartate, and a histidine. The latter two residues hydrogen bond to the nitrite and donate protons for the enzymatic reaction (14–18). In the absence of nitrite a water molecule occupies the fourth ligand position. Deprotonation of this water molecule occurs between pH 6 and 7 (18) and results in OH^- as the fourth ligand (19). NiR catalyzes the reduction of nitrite bidirectionally ($NO_2^- + e^- + 2H^+ \rightleftarrows NO + H_2O$) (20).

An important mechanistic question currently under debate (1) is whether nitrite binds to the oxidized type-2 copper first after which the electron is transferred to the type-2 site (5, 14, 21, 22) or whether the type-2 site is first reduced after which the nitrite binds to the copper (23–26). Also the possibility has been considered that the two routes operate in parallel (24, 26). Among key observations indicating that nitrite binds first to the oxidized copper are that the *reduced* type-2 site in NiR prefers a low occupancy of the fourth coordination position (14, 21, 22) and that the prereduced NiR only sluggishly reacts with nitrite (22, 27). On the other hand, in model complexes of the type-2 site, the copper is reduced prior to nitrite binding (28–30), and the nitrite dissociation constant of the oxidized type-2 site in NiR is more than 10-fold higher (25) than its Michaelis constant (K_m).

Here we report on investigations of the catalytic mechanism of NiR by kinetic techniques for which solutions of NiR with three different electron donors at saturating concentrations have been employed. The experiments have been complemented by electrochemical experiments on NiR that was immobilized on a rotating disk graphite electrode. It appears that the results can be analyzed and fitted satisfactorily on the basis of a random sequential mechanism.

EXPERIMENTAL PROCEDURES

Material—Wild-type NiR (from *Alcaligenes faecalis* S-6) and NiR M150T were prepared as described (20).[4] The copper content of native NiR and NiR M150T used for electrode experiments was 1.7 copper/monomer, as determined by the bicinchoninic acid method (32). For assays in solution, native NiR with a copper content of 2.0 per monomer was used.

Activity Assays in Solution—Unless reported otherwise, the buffer was 25 mM malate-MES-HEPES (MMH). The pH was adjusted with

* The costs of publication of this article were defrayed in part by the payment of page charges. This article must therefore be hereby marked "*advertisement*" in accordance with 18 U.S.C. Section 1734 solely to indicate this fact.

[S] The on-line version of this article (available at http://www.jbc.org) contains supplemental Table S1, Fig. S1, equations, and a supplemental scheme.

[1] Present address: Duke University, Medical Center, Dept. of Biochemistry, Durham, NC 27710.

[2] To whom correspondence should be addressed. E-mail: Canters@chem.leidenuniv.nl.

[3] The abbreviations used are: NiR, nitrite reductase; MES, 4-morpholineethanesulfonic acid; NHE, normal hydrogen electrode; HMM, Henri-Michaelis-Menten; wt, wild type.

[4] H. J. Wijma, I. MacPherson, M. Alexandre, R. E. M. Diederix, G. W. Canters, M. E. P. Murphy, and M. P. Verbeet, submitted for publication.

NaOH. Reported pH values are those of the assay buffer and were determined at the temperature of the assay. Nitrite reductase activity assays using saturating concentrations of reduced pseudoazurin (400 μM, which is well above K_m) as the electron donor were carried out as described (20) at 25 °C. The activity was measured by monitoring the increase of the absorption band at 590 nm, typical of oxidized pseudoazurin ($\varepsilon_{590\,nm} = 2900\ M^{-1}\ cm^{-1}$ (33)). A linear increase of absorbance with time (providing real initial rates) was observed in all cases.

Activity assays that employed benzyl viologen as the electron donor at saturating concentrations were carried out at 25 °C in a sealed cuvette that had been flushed with argon to make it anaerobic. The benzyl viologen (200 μM) was reduced by dithionite to an initial absorbance at 600 nm of 1.2–1.6. Alternatively, reduced benzyl viologen was prepared electrochemically with a platinum working electrode and an auxiliary electrode (34). The catalytic activity was calculated from the rate of decrease in absorbance of reduced benzyl viologen ($\varepsilon_{603\,nm} = 14{,}500\ M^{-1}\ cm^{-1}$ (35)) after addition of NiR, corrected for baseline drift. The decrease in absorbance was linear with respect to time after addition of NiR and remained so until >95% of the reduced viologen had been oxidized.

The activity with benzyl viologen as an electron donor was higher than the activity determined from the rate of reduction of nitrite (results not shown). This discrepancy arises because the nitric oxide product is reduced further, non-enzymatically, by the viologen to give nitrous oxide or ammonia (1). Because the stoichiometry between nitrite conversion and viologen consumption depended on the precise reaction conditions and varied from case to case (not further investigated) the catalytic activity is reported in arbitrary units when benzyl viologen was used as a reductant (see for instance Figs. 1*C* and 3*B*, *a.u.*). In some assays methyl viologen was used instead of benzyl viologen. The activities with a viologen as the electron donor, as quantified by nitrite disappearance, are similar to the activities with pseudoazurin as the electron donor (for *A. faecalis* S-6 NiR at pH 7 the k_{cat} of nitrite reduction is 338 s^{-1} with methyl viologen (36) and 392 s^{-1} with pseudoazurin (20) as the electron donor).

Activity Assays with a Rotating Disk Electrode—Activity assays employing a pyrolytic graphite edge electrode were carried out in an anaerobic cell (Metrohm) provided with an AUTOLAB rotating disk electrode (Eco Chemie), a platinum counter electrode, and an isothermal calomel electrode. During the experiments, the cell was kept anaerobic by flushing the head space with argon. The pyrolytic graphite edge electrode, constructed in the laboratory, had a surface area of 4 mm^2. Pyrolytic graphite (GE Advanced Ceramics) was embedded in epoxy (Araldite CY1300:HY1300 mixed 3:1 w/w from Ciba/Robnor) so that the basal plane was perpendicular with respect to the surface that contacts the solution. For NiR immobilization, the pyrolytic graphite edge electrode was polished thoroughly using a polishing cloth (Buehler) covered with 6 micron diamond, sonicated in H_2O, washed with buffer, then exposed to NiR (>100 μM) for ~30 s, rinsed with H_2O, and inserted in the buffer. After sealing the cell, the electrode was cycled between 560 and −140 mV *versus* normal hydrogen electrode (NHE) to check that oxygen was absent. Observed currents were corrected for background currents measured in the absence of nitrite.

Experiments were initiated by holding the electrode at a potential of 560 mV *versus* NHE for 10 s, followed by a "jump" to the desired value. After the background current had stabilized, the dependence of activity on nitrite concentration was measured by stepwise increases in nitrite concentration. The current at each nitrite concentration was averaged over 10 s, and the current in the absence of nitrite was subtracted. The temperature was kept at 0 °C to improve the stability of the protein film on the electrode; from control experiments it was established that the loss of active coverage during the time of the experiment was <10%.

For reliable determination of enzymatic constants by PFV, the electrode rotation rate should be sufficiently fast to prevent transport of substrate to the electrode (or accumulation of product near the electrode) becoming rate-limiting (37). Varying the rate of rotation between 500 and 9000 rpm did not influence the catalytic current, not even at the lowest nitrite concentrations. Thus, the catalytically active coverage of NiR on the electrodes is sufficiently low to maintain steady-state levels of substrate close to the surface of the electrode during turnover. Also the low currents observed (~300 nA) were consistent with a low catalytically active coverage. The coverage was estimated by assuming that the turnover rate/active site (k_t) is the same as measured in solution and is linearly related to the catalytic current (i_t) by Equation 1, $i_t = -FA\Gamma k_t$ (Equation 1), in which A is the surface area of the electrode, Γ is the enzymatic coverage (catalytically active subunits/unit of surface), F is the Faraday constant, and a negative sign signifies a reduction reaction. By combining the data from Figs. 1 and 4 the enzymatic coverage was estimated from Equation 1 to be 0.03 pmol cm^{-2}. As a comparison, for fumarate reductase (38) no transport limitation is observed at the much higher coverage of 13 pmol cm^{-2}. Also for hydrogenase (39), a far more active enzyme, no substrate depletion is observed provided the coverage is below 1 pmol cm^{-2}. These observations justify the assumption that in our case no complications because of transport limitations affect the observations. The typical rotation speed during the experiments was 2000 rpm. The data were fitted using Igor Pro (WaveMetrics, Inc.).

Modeling—The experimental results (see above) were analyzed on the basis of Scheme 1. Depicted are the type-2 site and the various changes it may undergo during turnover. In the starting configuration the oxidized Cu(II) carries water as the fourth ligand. Replacement of the water (step 1, k_1 and k_{-1}) by nitrite and subsequent electron transfer from the type-1 site to the type-2 site (step 3, k_3 and k_{-3}) leads to the reduced nitrite-bound type-2 site. These two steps constitute the B route. The A route consists of step 2 (electron transfer from type-1 to type-2) and the subsequent step 4 (nitrite binding) and leads to the same nitrite-bound reduced type-2 site, which is subsequently returned to the initial state (step 6) by conversion of nitrite to NO, dissociation of the NO, and binding of a water molecule. Conversion of the H_2O-bound reduced type-2 site to an inactive three-coordinate (14, 22) reduced form (step 5) is included in the scheme. The effect of this step (or equilibrium) on the reaction kinetics can be observed with freshly prepared enzyme in the initial phase of the reaction.[5] Scheme 1 applies at low pH; at high pH the same scheme applies but with the water replaced by OH^-. This also means that the kinetic constants in Scheme 1 are pH-dependent. In a random sequential mechanism as in Scheme 1, at low nitrite concentration electron transfer to the type-2 site will be faster than nitrite binding, and catalysis will mainly occur via the A route (step 2 and 4). At higher nitrite concentration, the nitrite binding will become faster than the electron transfer to the H_2O/OH^--bound type-2 site, and catalysis will follow the B route (via steps 1 and 3).

When Scheme 1 applies the dependence of k_t on the nitrite concentration ([S]) can be shown to obey Equation 2 (see supplemental materials for derivation and details), $k_t(S) = (k_{cat}^A[S] + k_{cat}^B[S]^2/K_m^B)/(K_m^A + [S] + [S]^2/K_m^B)$ (Equation 2). Equation 2 also applies when the isomerization (step 5) is omitted from Scheme 1. The terms k_{cat}^A and K_m^A, and k_{cat}^B and K_m^B are primarily associated with the A and B routes, respectively. Thus, the Michaelis constants K_m^A and K_m^B are a measure of K_d^{red} (k_{-1}/k_1) and K_d^{ox} (k_{-4}/k_4),

[5] H. J. Wijma, L. J. C. Jeuken, M. P. Verbeet, F. A. Armstrong, and G. W. Canters, unpublished results.

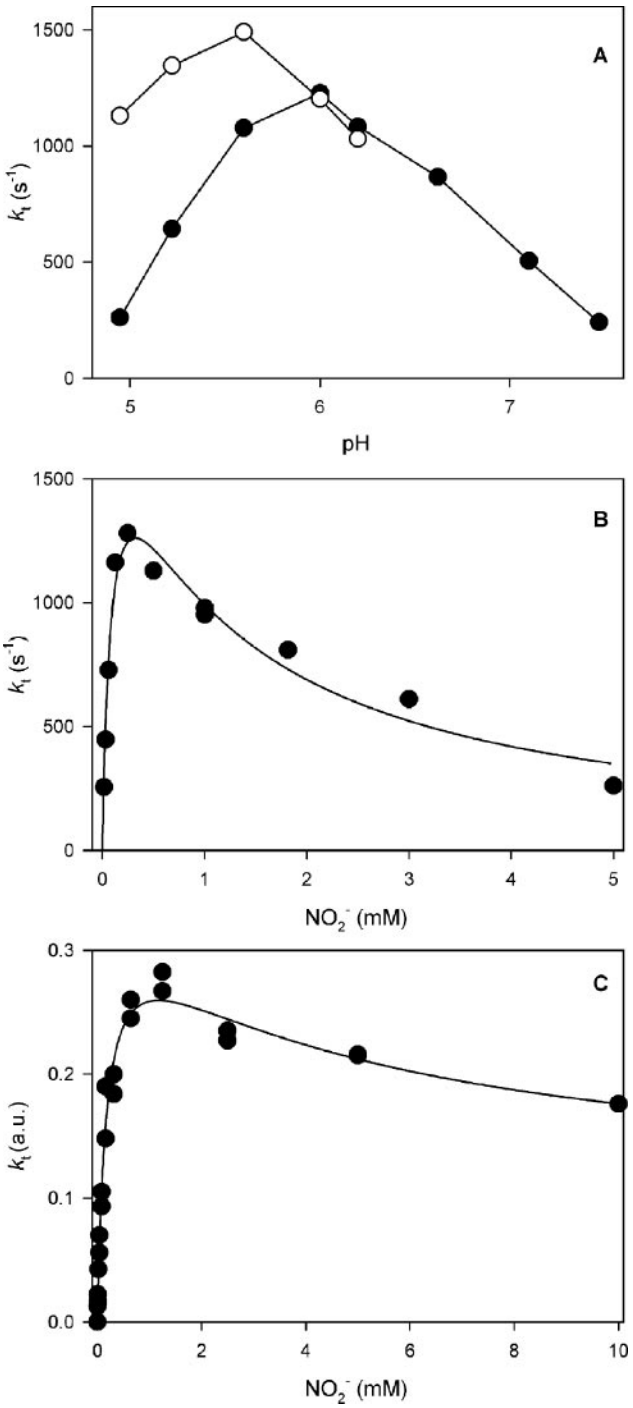

FIGURE 1. **Dependence of catalytic activity on pH and nitrite concentration.** *A*, activity *versus* pH with pseudoazurin as the electron donor. The *filled circles* refer to data obtained in the presence of 5 mM nitrite, and the *open circles* correspond to 500 μM nitrite. The lines merely connect the points, they are not a fit. The buffer was 25 mM malate-MES-HEPES set at pH with NaOH; the temperature was 25 °C. *B*, activity *versus* nitrite concentration with pseudoazurin as the electron donor at pH 4.9. The *solid line* is a fit of the data to Equation 2 yielding $k_{cat}^{A} = 2114 \pm 426\ s^{-1}$, $k_{cat}^{B} < 690\ s^{-1}$, $K_m^{A} = 98 \pm 29\ \mu M$, $K_m^{B} = 1.07 \pm 0.51$ mM. *C*, activity *versus* nitrite concentration with benzyl viologen as the electron donor at pH 5.4. The *solid line* is a least-squares fit to Equation 2 resulting in $k_{cat}^{B}/k_{cat}^{A} = 0.29 \pm 0.21$, $K_m^{A} = 184 \pm 37\ \mu M$, $K_m^{B} = 4470 \pm 3510\ \mu M$. *a.u.*, arbitrary units.

respectively. Michaelis constants approximate to dissociation constants when (*a*) the catalytic step is much faster than the electron-transfer steps, (*b*) the isomerization (step 5) is slow, and (*c*) the dissociation of nitrite is faster than the other steps (see Table S1 in supplemental material). Furthermore, when step 6 is not rate-limiting we find that (Table S1 in supplemental material) the ratio of k_{cat}^{B}/k_{cat}^{A} approximately equals the ratio of the electron transfer rates k_3 and k_2. In the case that NiR follows an ordered mechanism (only steps 2, 4, and 6 or only steps 1, 3, 5, and 6) standard Henri-Michaelis-Menten (HMM) behavior should be observed, as given by $k_t(S) = k_{cat}[S]/(K_m + [S])$ (Equation 3).

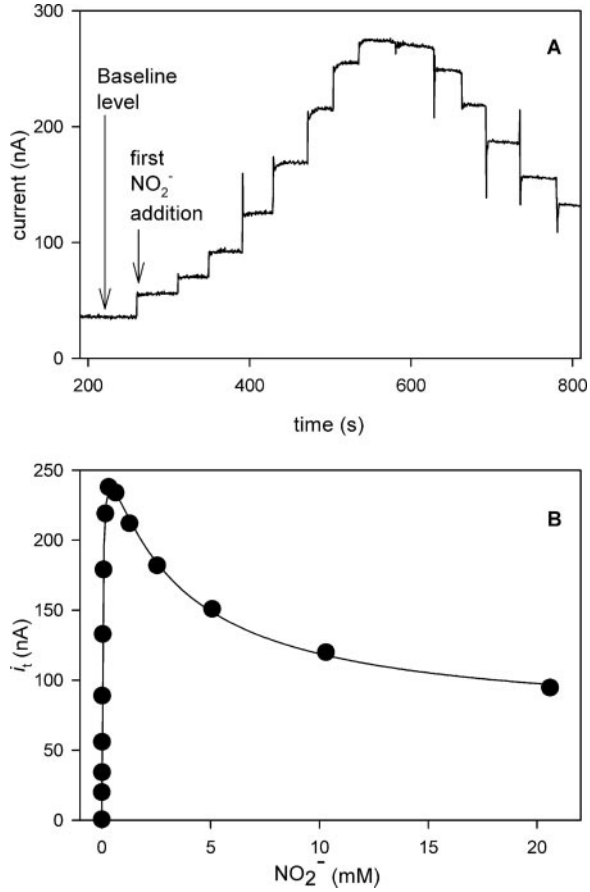

FIGURE 2. **Kinetic constants measured by protein film voltammetry.** *A*, reductive current *versus* time upon subsequent nitrite additions. After the electrode was held at −70 mV *versus* NHE for 200 s, the background current was stable, and the nitrite concentration was increased stepwise. *B*, plot of the baseline-subtracted reductive current *versus* concentration of nitrite at pH 5.7. The *solid line* is a fit to Equation 2 and yielded $k_{cat}^{B}/k_{cat}^{A} = 0.25 \pm 0.02$, $K_m^{A} = 43 \pm 2\ \mu M$, $K_m^{B} = 2961 \pm 273\ \mu M$. The buffer was 25 mM malate-MES-HEPES at 0 °C. For experimental details see "Experimental Procedures."

RESULTS

Deviations from Henri-Michaelis-Menten Kinetics by NiR—The investigations were started by measuring the catalytic activity (k_t) of nitrite reductase as a function of pH with pseudoazurin as the electron donor at saturating concentrations. With 500 μM nitrite maximum activity was observed around pH 5.6, whereas at 5 mM nitrite maximum activity occurred at pH 6.0 (Fig. 1*A*). Interestingly, the maximum activity was 25% higher with 500 μM nitrite than with 5 mM nitrite. To investigate this phenomenon further, we assayed the activity as a function of nitrite concentration. At pH 4.9, the activity with increasing nitrite concentration reached a maximum followed by a steady decrease at higher nitrite concentrations (Fig. 1*B*) that could be fitted to Equation 2 resulting in $k_{cat}^{B}/k_{cat}^{A} < 0.4$.

To investigate the possible dependence of these kinetics on the nature of the electron donor, we used benzyl viologen instead of pseudoazurin, again at saturating concentrations. Benzyl viologen is a far stronger reductant ($E_M = -350$ mV *versus* NHE) than pseudoazurin ($E_M = 295$ mV at pH 6 (20)). Furthermore, benzyl viologen is expected to reduce

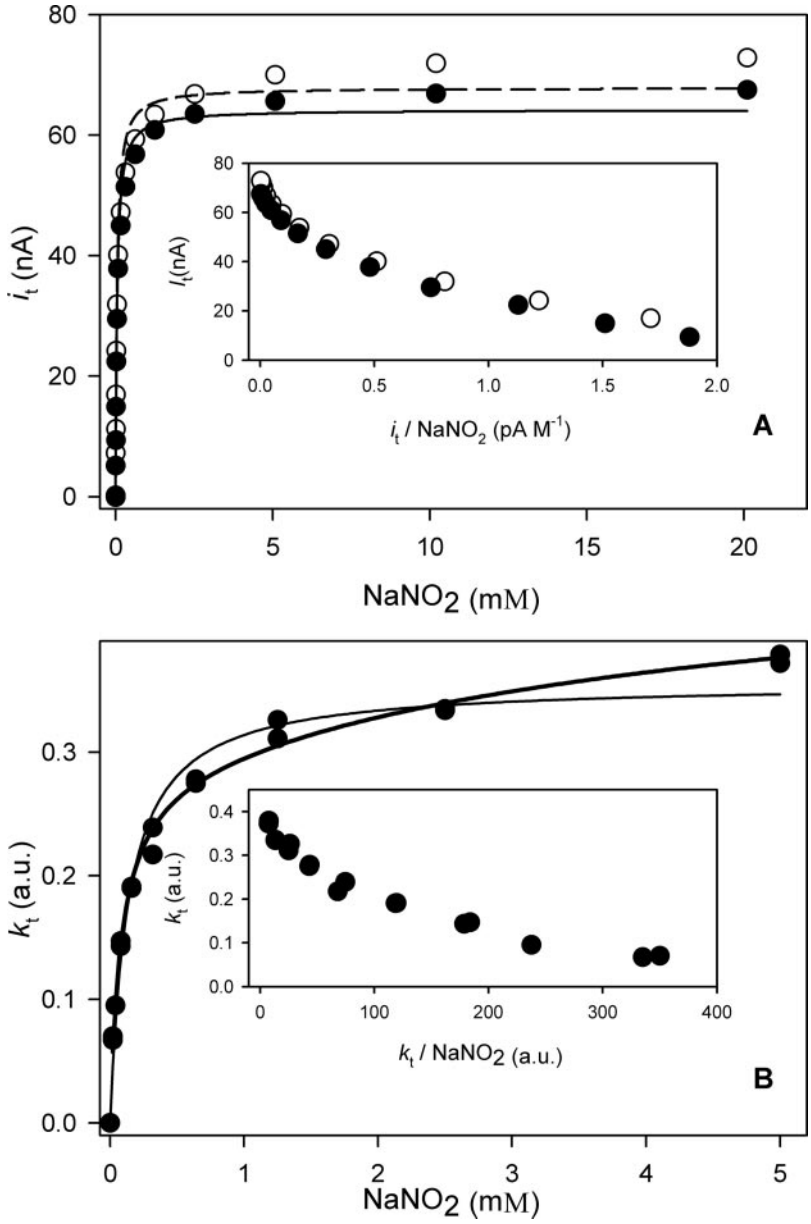

FIGURE 3. **Deviations from Henri-Michaelis-Menten kinetics at high pH.** *A*, activity *versus* nitrite concentration of two different batches of native NiR immobilized on a pyrolytic graphite edge electrode. *Closed* and *open circles* represent the different batches that are fitted to the Henri-Michaelis-Menten equation (Equation 3) by a *continuous* and a *broken line*, respectively. The two fits resulted in K_m values of 47 ± 6 μM and 48 ± 5 μM (at pH 7.47). The *inset* shows the Eadie-Hofstee plot in which all points should lie on straight line were the Henri-Michaelis-Menten equation to be obeyed. The *y* axis in the Eadie-Hofstee plot is activity, the *x* axis is activity divided by substrate concentration. *B*, activity *versus* nitrite concentration at pH 7.14 with benzyl viologen as electron donor. Shown is a fit to the Henri-Michaelis-Menten Equation 3 (THIN *solid line*) and to Equation 2 (*thick line*, $k^B_{cat}/k^A_{cat} > 1.3$, $K^A_m = 79 \pm 12$ μM, $K^B_m >$ 5000 μM, within the range of accessible nitrite concentrations (< 5 mM) no saturation of the rate occurred, meaning only lower estimates of k^B_{cat}/k^A_{cat} and K^B_m are possible).

NiR via a nonspecific collisional mechanism, whereas pseudoazurin forms a specific complex with NiR (40–42), so we might also ascertain the role of complex formation in the overall mechanism. Our results showed that with benzyl viologen as the electron donor, the catalytic rate also diminished at higher nitrite concentrations (Fig. 1*C*).

Finally, in a separate experiment the catalytic activity of NiR immobilized on a rotating disk electrode was measured by observing the reductive current (Fig. 2*A*). The activity displayed the same dependence on nitrite concentration (Fig. 2*B*) as observed before in the bulk experiments, both at electrode potentials of −70 and +110 mV *versus* NHE. The latter observation shows that the measured activities do not depend on the kinetics of the electron transfer between electrode and type-1 site. If the experiment was started at high nitrite concentration, and the solution was diluted, an increase in catalytic current was observed (results not shown). In addition, the M150T mutant of NiR (in which intramolecular electron transfer from type-1 to type-2 is retarded), also displayed a decrease in i_{cat} at higher nitrite concentrations (Fig. S1 of supplemental materials). Thus, it was established that regardless of the nature of the electron donor the catalytic activity of NiR is optimized at a particular nitrite concentration and drops when this level is exceeded.

TABLE 1

Effect of pH on kinetic constants of NiR in solution assays

The reported errors are S.D. BV-SDT, benzyl viologen reduced *in situ* by sodium dithionite; BV, reduced benzyl viologen was prepared electrochemically. See "Experimental Procedures" for experimental details.

Electron donor	pH	k^B_{cat}/k^A_{cat}	K^A_m	K^B_m
			μM	μM
Pseudoazurin	4.9	<0.41	98 ± 29	1,070 ± 510
BV-SDT	4.6	<0.22	124 ± 22	389 ± 97
BV-SDT	5.4	0.29 ± 0.21	184 ± 37	4,470 ± 3510
BV-SDT	6.4	>1	152 ± 22	>10,000
BV	7.1	>1	79 ± 12	>5,000

Equation 2 not only accounted for the kinetic data obtained below pH 6.5 but gave a better fit than the HMM Equation 3 at higher pH. At higher nitrite concentrations the best fits to Equation 3 deviate significantly from the experimental points (Fig. 3*A*, only fits to Equation 3 are shown). To check whether the observed extra activity at high nitrite

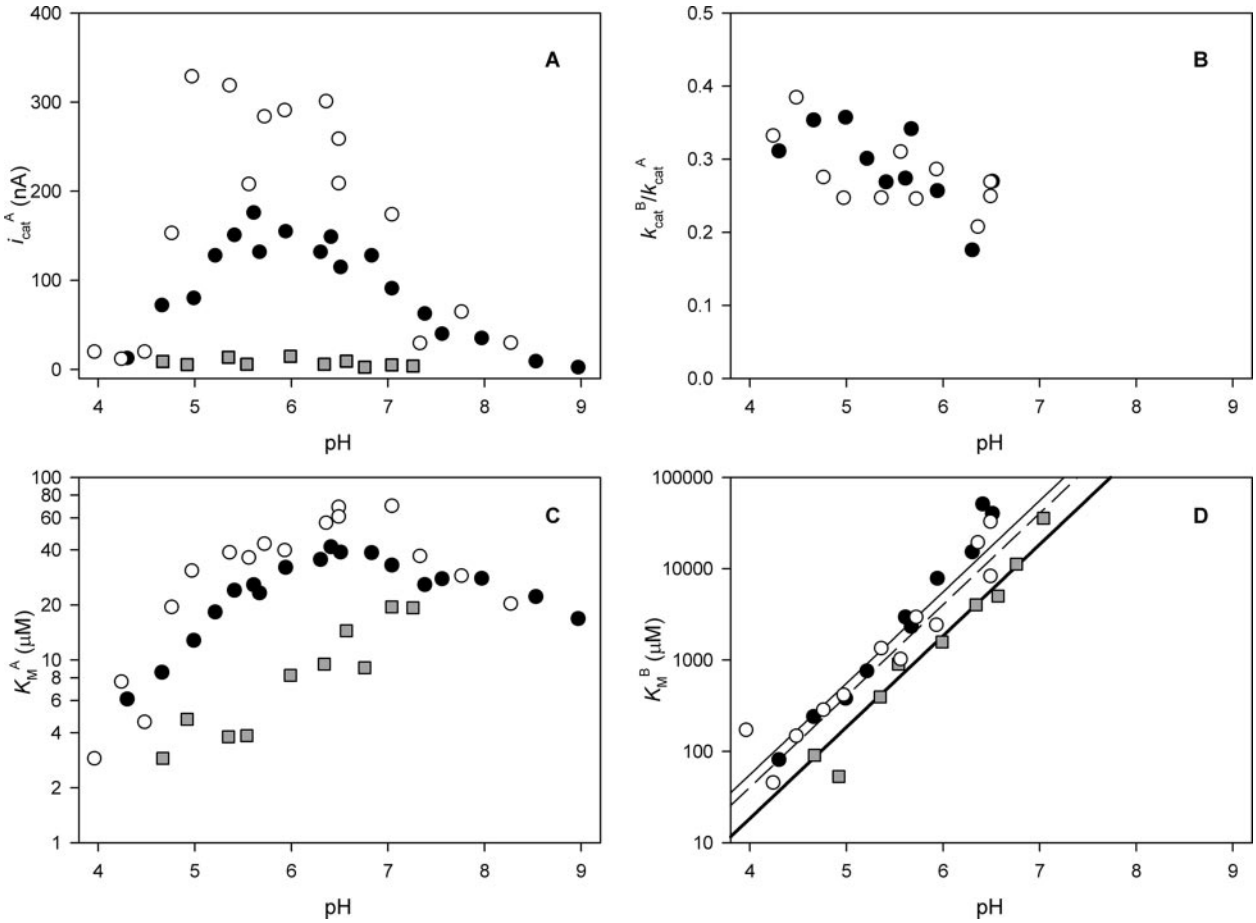

FIGURE 4. **Kinetic constants of electrode-immobilized NiR *versus* pH.** *Open circles* denote the kinetic constants of wt NiR determined on a pyrolytic graphite edge electrode held at −70 mV *versus* NHE, *closed circles* denote those determined at +110 mV *versus* NHE, and *gray-filled squares* denote the data points of NiR M150T determined at −70 mV *versus* NHE (no data points are shown in *B* because i_{cat}^{B} was difficult to determine because of the low amplitude). The *thin line* in *D* is a linear fit of log K_m^B *versus* pH of the data points at +110 mV, the *dashed line* is a fit to the data points at −70 mV for wt, and the *thick line* is a fit to the data points of M150T. In *B* and *D* no data points are shown above pH 7 because above this pH no saturation is observed and thus no data could be obtained. *A*, i_{cat}^{A} *versus* pH; *B*, k_{cat}^{B}/k_{cat}^{A} *versus* pH; *C*, K_m^A *versus* pH; *D*, K_m^B *versus* pH.

concentration was not caused by a co-purified contaminant (such as proteolytically degraded enzyme or redox-active metal ions) two independent batches of NiR were used under otherwise identical conditions (Fig. 3*A*). Both batches gave the same deviations from HMM kinetics (Fig. 3*A*) and, when fitted to the HMM equation, produced the same Michaelis constants (47 ± 6 μM and 48 ± 5 μM). Thus, the deviation from HMM kinetics is characteristic of the intact NiR and is not caused by a contaminant.

With benzyl viologen as electron donor, identical deviations from HMM occurred reproducibly above pH 6 (Fig. 3*B*; the *thin line* is a fit according to HMM kinetics, Table 1). An Eadie-Hofstee plot, in which deviations from HMM kinetics appear as deviations from linearity, showed the same, non-linear, trends for assays on the electrode and in solution (Fig. 3, *A* and *B*, *insets*). It was possible, however, to fit the activity *versus* nitrite concentration to Equation 2 (Fig. 3*B*, *thick line*, and Table 1). Also for NiR M150T a substrate activation-like phenomenon occurred (results not shown). Thus, over the measured pH range the data are fit most satisfactorily assuming a random-sequential mechanism according to Equation 2. Because $k_{cat}^{B} < k_{cat}^{A}$ below pH 6.5 and $k_{cat}^{B} > k_{cat}^{A}$ above pH 6.5 (Table 1), it appears that electron transfer to the type-2 site is retarded if nitrite replaces a water molecule (below pH 6.5) but becomes faster above pH 6.5 where the nitrite replaces a hydroxyl ion.

Kinetic Constants Versus pH—At the rotating disk electrode, a far lower background activity was observed than in solution assays, which made it possible to measure, accurately, K_m^A, K_m^B, and the ratio of k_{cat}^{B}/k_{cat}^{A} over a wide pH range (Fig. 4). The individual trends of k_{cat}^{A} and k_{cat}^{B} *versus* pH could not be determined accurately because the currents depended on the enzymatic coverage, which was only reproducible within 50% between different protein films (this is not apparent in Fig. 3*A* where results are reported on two different samples, which happen to exhibit similar surface coverages, but it can be clearly seen in Fig. 4*A* where, *e.g.* around pH 5.5, i_{cat} varies from 200 to 325 nA for wt NiR at −70 mV *versus* NHE). Even so, a plot of i_{cat}^{A} (Equation 1) *versus* pH determined for wt NiR at +110 mV *versus* NHE (Fig. 4*A*, *closed circles*) agrees with the activity *versus* pH at 500 μM nitrite when pseudoazurin is used as the electron donor (Fig. 1*A*). Although the data points at −70 mV exhibit a larger spread a similar trend is still observed in this case. Above pH 9 the catalytic currents for wt NiR were too low to be observed, whereas below pH 4 the higher background activity and the lower catalytic currents of NiR prevented measurements. For NiR M150T the observed currents were far lower (Fig. 4*A*), and as a result the observable range was limited from pH 4.5 to 7.5.

The k_{cat}^{B}/k_{cat}^{A} ratio was ~0.3 below pH 6.5 (Fig. 4*B*), whereas above pH 7 k_{cat}^{B}/k_{cat}^{A} was >1 (results not shown, exact values could not be obtained because K_m^B is larger than the experimentally accessible range of nitrite concentration). Below pH 6.0 in bulk solution (Table 1), and for M150T on the electrode, most data points for k_{cat}^{B}/k_{cat}^{A} were less accurate because of difficulties with subtracting the background activity at high nitrite concentration. For M150T around pH 6.5, the ratios were

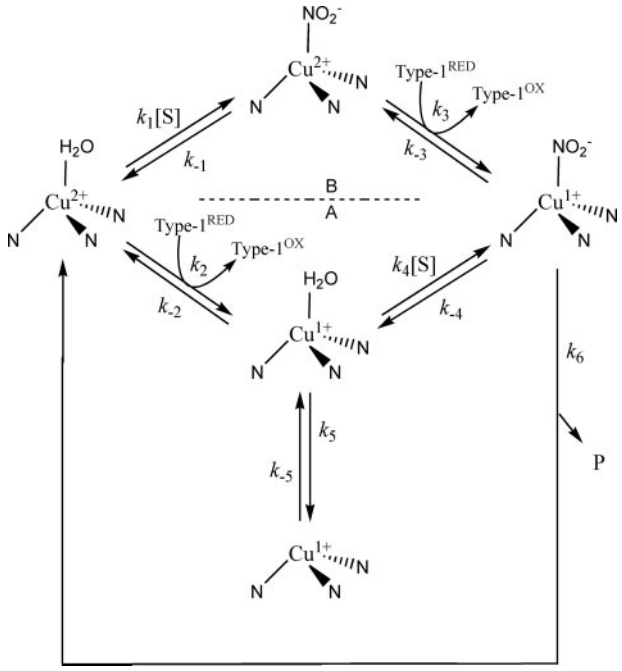

SCHEME 1. **Proposed catalytic mechanism of NiR.** The catalytic and product release step k_6 is in fact reversible (20), which is not modeled because in the current experiments the build-up of the product nitric oxide is prevented. The nitrite is depicted as deprotonated but it may also be protonated in the catalytic cycle.

approximately the same as for the wt NiR (at pH 6.76 the ratio was 0.46, and at pH 6.57 it was 0.36).

For M150T the K_m^A was 2–10-fold lower than for wt NiR (Fig. 4*C*). A plot of log K_m^B *versus* pH (Fig. 4*D*) revealed a slope of 1 for both wt NiR and NiR M150T. For wt, there was no significant difference between the K_m^B values at −70 mV and at 110 mV. The values of M150T were two times lower than those of the wt NiR at the same electrode potential. The logarithmic plot of the solution data of K_m^B *versus* pH also displays a slope of ~1 (Table 1).

DISCUSSION

Random-sequential Mechanism—The simplest explanation for our data invokes a random-sequential mechanism that accounts for nitrite binding and type-2 site reduction (Scheme 1). At low nitrite concentration, reduction of the type-2 site is faster than nitrite binding to the oxidized site (A route), whereas at high nitrite concentrations the binding is faster and the reaction is diverted through the B route. Below pH 6.5, we find that the B route is slower than the A route (indicated by $k_{cat}^B/k_{cat}^A < 1$) because the rate-limiting step of electron transfer to the type-2 site is slower with nitrite-bound than with H_2O-bound, in agreement with literature reports that electron transfer from the type-1 to the type-2 site is slower in the presence of nitrite (43–46) and that electron transfer is a rate-limiting step for turnover of the NiR (18, 44, 47). Above pH 6.5, the B route is faster than the A route ($k_{cat}^B/k_{cat}^A > 1$), because the type-2 H_2O ligand (which is easily substituted by nitrite) is replaced by/converted to OH^- (18, 19), and electron transfer to the type-2 site is faster with nitrite bound than with OH^- (Table 1, Fig. 3). Also, the absolute magnitude and pH dependence of K_m^B, which corresponds to the nitrite binding step in Scheme 1 (step 1), agrees with the K_d^{ox} for nitrite (see above), consistent with the random-sequential mechanism. In the next three paragraphs we consider a number of alternatives to explain our data.

According to an ordered mechanism electron transfer from type-1 to type-2 occurs to either the H_2O/OH^--bound or the nitrite-bound type-2 site. Such a sharp division is not observed in pulse-radiolysis experiments (43–46). Secondly, with assays employing a strong and fast electron donor, like benzyl viologen or methyl viologen, it is expected that at low nitrite concentrations a large proportion of the NiR will have both the type-1 and the type-2 site reduced. With viologens as the electron donor, the K_m^A (Table 1) and k_{cat} values of NiR (see "Experimental Procedures") are similar to those found in the presence of the physiological electron donor, which is only able to reduce the type-1 site. This observation suggests that nitrite can bind to the reduced type-2 site and that the "nitrite-binds-prior-to-reduction" ordered mechanism does not apply. Assuming a random-sequential mechanism also obviates the need to postulate the existence of a sensor loop between type-1 and type-2 site (22, 48).

An alternative explanation for the observed substrate inhibition could be that a second nitrite may bind to the type-2 site (Scheme S1 in supplemental materials). We can rule out this possibility on the basis of the available crystallographic evidence. In nine crystal structures of oxidized NiR and five crystal structures of reduced NiR (16, 21, 49–53) only one nitrite is found at the type-2 site.

Against a "reduction-before-nitrite-binding" ordered mechanism (thereby supporting a nitrite-binding-prior-to-reduction ordered mechanism) it has been argued that reduction of type-2 site before nitrite binding may result in a three-coordinated inactive form (22). We have data[5] indicating that after a reduction of the type-2 site a slow reversible isomerization to a reduced inactive form may occur (Scheme 1, step 5). However this step is slow compared with step 4 at nitrite concentrations above K_d^{red}, and the possible occurrence of this state is still compatible with a random-sequential mechanism.

The Effect of pH and Nitrite Concentration on Catalysis—Our data on the pH dependence of the catalytic activity of NiR (Fig. 1) are in agreement with literature data (54). Also our K_m^A value at pH 7 (79 ± 12 μM) with benzyl viologen as the electron donor agrees with the value of 74 μM determined by Kakutani *et al.* (54) with methyl viologen as the electron donor.

In this work, for the first time the effect of nitrite concentration on the activity at low pH is studied. An all determining factor is the logarithmic dependence of K_m^B on pH, *i.e.* the affinity constant for the B route. Our data show that below pH 6 the K_m^B becomes low enough that at typical assay conditions (~1 mM nitrite) catalysis via the B route begins to prevail, resulting in a drop in activity (indicated by $k_{cat}^B < k_{cat}^A$, Fig. 4*B*). Above pH 6, the K_m^B is so high that in typical activity assays most catalysis occurs via the A route. Thus, from pH 6 to pH 5 the loss of activity observed in plots of activity *versus* pH (17, 18, 25, 54, 55), can be assigned to the increasing prevalence of the slower B route. Below pH 5 the k_{cat}^A and k_{cat}^B values drop dramatically and at pH < 4 they fall below the detection limit (Fig. 4*A*). The simplest explanation for this is that the type-1 to type-2 electron transfer rate decreases below this pH, as it does in related nitrite reductases (44).

A key feature of Scheme 1, in agreement with literature data (43–46) is that the rate-limiting electron transfer rate between type-1 and type-2 site depends on the ligand that is bound to the type-2 site. The rates decrease in the order H_2O > nitrite > OH^-. The slower electron transfer to the type-2 site with nitrite/OH^- bound may be because of a lower midpoint potential of the type-2 site and/or a higher reorganization energy (56) than with H_2O as a ligand. In fact in pulse-radiolysis experiments a 100-mV decrease in type-2 site midpoint potential is found when the pH is raised from 6 to 8 (44).

The up to 10 times lower values of K_m^A for NiR M150T illustrate the dependence of this parameter on the electron-transfer kinetics. With slower electron transfer,[5] K_m will decrease because saturation will occur

at lower nitrite concentration. It appears that the effect of a slower electron transfer rate is more pronounced for K_m^A (Fig. 4*C*) than for K_m^B (Fig. 4*D*), whereas K_m^A also follows a complicated behavior *versus* pH (for a simple protonation/deprotonation equilibrium slopes equal to 1, 0, or −1 are expected in a logarithmic plot). Apparently K_m^B is less sensitive than K_m^A to the various kinetic parameters in the system and thus provides a better probe of nitrite binding.

The linear dependence of log K_m^B on pH suggests that either a chemical group in NiR or nitrite itself needs to be protonated before catalysis and because no leveling off is observed that the pK_a is < 4.5. The corresponding acid could be the nitrite (pK_a = 3.25), the active site aspartate (usual pK_a range in proteins (31) is 2–5.5) that is known to hydrogen bond to the bound nitrite (14, 16, 18), or the active site His-255 (usual range for histidine is 5–8). The linear dependence of log K_m^B on pH is similar to that found (25) for the K_d^{ox} value of the type-2 site of *Alcaligenes xylosoxidans* NiR (in frozen samples < 30 μM at pH 5.2, 350 μM at pH 7.5). EPR experiments on *A. faecalis* S-6 NiR as a function of pH[6] have shown that the K_d^{ox} for the type-2 site (≈1 mM at pH 6, ≈10 mM at pH 7 in frozen samples) is indeed approximately equal to the K_m^B (see Fig. 4*D*).

Conclusions—A random-sequential mechanism is in agreement with the steady-state kinetics observed for wt and M150T NiR with all tested electron donors. At low nitrite concentration, electron transfer occurs prior to nitrite binding, whereas at higher nitrite concentration nitrite binding occurs first. The velocity of the rate-limiting electron transfer step between the type-1 and the type-2 site depends on the ligand that is bound at the type-2 site and decreases in the order H_2O > nitrite > OH^-. The K_m^B and K_d^{ox} values of NiR are similar and show a normal pH dependence with p$K_a < 4.5$. The results are in agreement with NiR as a robust machinery that can effectively bind nitrite and catalyze its reduction over a wide range of nitrite concentration and pH.

Acknowledgments—We thank Dr. H. A. Heering and Dr. A. W. J. W. Tepper for useful discussions, Dr. K. Vincent for help with some electrochemical experiments, and R. Zwier for manufacturing excellent equipment.

REFERENCES

1. Zumft, W. G. (1997) *Microbiol. Mol. Biol. Rev.* **61,** 533–616
2. Bange, H. W. (2000) *Nature* **408,** 301–302
3. Robertson, G. P., Paul, E. A., and Harwood, R. R. (2000) *Science* **289,** 1922–1925
4. Ichiki, H., Tanaka, Y., Mochizuki, K., Yoshimatsu, K., Sakurai, T., and Fujiwara, T. (2001) *J. Bacteriol.* **183,** 4149–4156
5. Adman, E. T., and Murphy, M. E. P. (2001) in *Handbook of Metalloproteins* (Messerschmidt, A., Huber, R., Poulos, T., Wieghardt, K., eds), pp. 1381–1390, John Wiley & Sons, Ltd., Chicester
6. Cardinale, J. A., and Clark, V. L. (2000) *Infect. Immun.* **68,** 4368–4369
7. Rock, J. D., and Moir, J. W. (2005) *Biochem. Soc. Trans.* **33,** 134–136
8. Sasaki, S., Karube, I., Hirota, N., Arikawa, Y., Nishiyama, M., Kukimoto, M., Horinouchi, S., and Beppu, T. (1998) *Biosens. Bioelectron.* **13,** 1–5
9. Wu, Q., Storrier, G. D., Pariente, F., Wang, Y., Shapleigh, J. P., and Abruña, H. D. (1997) *Anal. Chem.* **69,** 4856–4863
10. Astier, Y., Canters, G. W., Davis, J. J., Hill, H. A. O., Verbeet, M. P., and Wijma, H. J. (2005) *Chem. Phys. Chem.* **6,** 1114–1120
11. Libby, E., and Averill, B. A. (1992) *Biochem. Biophys. Res. Commun.* **187,** 1529–1535
12. Godden, J. W., Turley, S., Teller, D. C., Adman, E. T., Liu, M. Y., Payne, W. J., and LeGall, J. (1991) *Science* **253,** 438–442
13. Kukimoto, M., Nishiyama, M., Murphy, M. E., Turley, S., Adman, E. T., Horinouchi, S., and Beppu, T. (1994) *Biochemistry* **33,** 5246–5252
14. Murphy, M. E., Turley, S., and Adman, E. T. (1997) *J. Biol. Chem.* **272,** 28455–28460
15. Boulanger, M. J., Kukimoto, M., Nishiyama, M., Horinouchi, S., and Murphy, M. E. (2000) *J. Biol. Chem.* **275,** 23957–23964
16. Boulanger, M. J., and Murphy, M. E. (2001) *Biochemistry* **40,** 9132–9141
17. Kataoka, K., Furusawa, H., Takagi, K., Yamaguchi, K., and Suzuki, S. (2000) *J. Biochem.* (*Tokyo*) **127,** 345–350
18. Zhao, Y., Lukoyanov, D. A., Toropov, Y. V., Wu, K., Shapleigh, J. P., and Scholes, C. P. (2002) *Biochemistry* **41,** 7464–7474
19. Ellis, M. J., Dodd, F. E., Strange, R. W., Prudencio, M., Sawers, G., Eady, R. R., and Hasnain, S. S. (2001) *Acta. Crystallogr. Sect. D Biol. Crystallogr.* **57,** 1110–1118
20. Wijma, H. J., Canters, G. W., de Vries, S., and Verbeet, M. P. (2004) *Biochemistry* **43,** 10467–10474
21. Adman, E. T., Godden, J. W., and Turley, S. (1995) *J. Biol. Chem.* **270,** 27458–27474
22. Strange, R. W., Murphy, L. M., Dodd, F. E., Abraham, Z. H., Eady, R. R., Smith, B. E., and Hasnain, S. S. (1999) *J. Mol. Biol.* **287,** 1001–1009
23. Hulse, C. L., and Averill, B. A. (1989) *J. Am. Chem. Soc.* **111,** 2322–2323
24. Averill, B. A. (1996) *Chem. Rev.* **96,** 2951–2964
25. Abraham, Z. H., Smith, B. E., Howes, B. D., Lowe, D. J., and Eady, R. R. (1997) *Biochem. J.* **324,** 511–516
26. Wasser, I. M., de Vries, S., Moenne-Loccoz, P., Schroder, I., and Karlin, K. D. (2002) *Chem. Rev.* **102,** 1201–1234
27. Kashem, M. A., Dunford, H. B., Liu, M. Y., Payne, W. J., and LeGall, J. (1987) *Biochem. Biophys. Res. Commun.* **145,** 563–568
28. Halfen, J. A., Mahapatra, S., Olmstead, M. M., and Tolman, W. B. (1994) *J. Am. Chem. Soc.* **116,** 2173–2174
29. Casella, L., Carugo, O., Gulotti, M., Doldi, S., and Frassoni, M. (1996) *Inorg. Chem.* **35,** 1101–1113
30. Monzani, E., Anthony, G. J., Koolhaas, A., Spandre, A., Leggieri, E., Casella, L., Gulotti, M., Nardin, G., Randaccio, L., Fontani, M., Zanello, P., and Reedijk, J. (2000) *J. Biol. Inorg. Chem.* **5,** 251–261
31. Fersht, A. (1985) in *Enzyme Structure and Mechanism*, pp. 55, 133, 156, and 256, W. H. Freeman and Company, New York
32. Brenner, A. J., and Harris, E. D. (1995) *Anal. Biochem.* **226,** 80–84
33. Kakutani, T., Watanabe, H., Arima, K., and Beppu, T. (1981) *J. Biochem.* (*Tokyo*) **89,** 463–472
34. Stankovich, M. T. (1980) *Anal. Biochem.* **109,** 295–308
35. van Leeuwen, J. W., van Dijk, C., and Veeger, C. (1983) *Eur. J. Biochem.* **135,** 601–607
36. Wijma, H. J., Boulanger, M. J., Molon, A., Fittipaldi, M., Huber, M., Murphy, M. E., Verbeet, M. P., and Canters, G. W. (2003) *Biochemistry* **42,** 4075–4083
37. Heering, H. A., Hirst, J., and Armstrong, F. A. (1998) *J. Phys. Chem. B.* **102,** 6889–6902
38. Léger, C., Heffron, K., Pershad, H. R., Maklashina, E., Luna-Chavez, C., Cecchini, G., Ackrell, B. A., and Armstrong, F. A. (2001) *Biochemistry* **40,** 11234–11245
39. Jones, A. K., Lamle, S. E., Pershad, H. R., Vincent, K. A., Albracht, S. P. J., and Armstrong, F. A. (2003) *J. Am. Chem. Soc.* **125,** 8505–8514
40. Kukimoto, M., Nishiyama, M., Ohnuki, T., Turley, S., Adman, E. T., Horinouchi, S., and Beppu, T. (1995) *Protein Eng.* **8,** 153–158
41. Kukimoto, M., Nishiyama, M., Tanokura, M., Adman, E. T., and Horinouchi, S. (1996) *J. Biol. Chem.* **271,** 13680–13683
42. Impagliazzo, A., and Ubbink, M. (2004) *J. Am. Chem. Soc.* **126,** 5658–5659
43. Suzuki, S., Deligeer, Yamaguchi, K., Kataoka, K., Kobayashi, K., Tagawa, S., Kohzuma, T., Shidara, S., and Iwasaki, H. (1997) *J. Biol. Inorg. Chem.* **2,** 265–274
44. Kobayashi, K., Tagawa, S., Deligeer, and Suzuki, S. (1999) *J. Biochem.* (*Tokyo*) **126,** 408–412
45. Suzuki, S., Furusuwa, H., Kataoka, K., Yamaguchi, K., Kobayashi, K., and Tagawa, S. (2000) *Inorg. React. Mechan.* **2,** 129–135
46. Suzuki, S., kataoke, K, Yamaguchi, K, Inoue, T., and Kai, Y. (1999) *Coord. Chem. Rev.* **190–192,** 245–265
47. Deligeer, Fukunaga, R., Kataoka, K., Yamaguchi, K., Kobayashi, K., Tagawa, S., and Suzuki, S. (2002) *J. Inorg. Biochem.* **91,** 132–138
48. Hough, M. A., Ellis, M. J., Antonyuk, S., Strange, R. W., Sawers, G., Eady, R. R., and Hasnain, S. S. (2005) *J. Mol. Biol.* **350,** 300–309
49. Dodd, F. E., Hasnain, S. S., Abraham, Z. H. L., Eady, R. R., and Smith, B. E. (1997) *Acta Crystallogr. Sect. D* **53,** 406–418
50. Dodd, F. E., Van Beeumen, J., Eady, R. R., and Hasnain, S. S. (1998) *J. Mol. Biol.* **282,** 369–382
51. Tocheva, E. I., Rosell, F. I., Mauk, A. G., and Murphy, M. E. P. (2004) *Science* **304,** 867–870
52. Boulanger, M. J., and Murphy, M. E. P. (2003) *Protein Sci.* **12,** 248–256
53. Murphy, M. E., Turley, S., Kukimoto, M., Nishiyama, M., Horinouchi, S., Sasaki, H., Tanokura, M., and Adman, E. T. (1995) *Biochemistry* **34,** 12107–12117
54. Kakutani, T., Watanabe, H., Arima, K., and Beppu, T. (1981) *J. Biochem.* (*Tokyo*) **89,** 453–461
55. Iwasaki, H., and Matsubara, T. (1972) *J. Biochem.* (*Tokyo*) **71,** 645–652
56. Marcus, R. A., and Sutin, N. (1985) *Biochim. Biophys. Acta* **811,** 265–322

[6] M. Fittipaldi and H. J. Wÿma, unpublished results.

A Random-sequential Mechanism for Nitrite Binding and Active Site Reduction in Copper-containing Nitrite Reductase

Hein J. Wijma, Lars J. C. Jeuken, Martin P. Verbeet, Fraser A. Armstrong and Gerard W. Canters

J. Biol. Chem. 2006, 281:16340-16346.
doi: 10.1074/jbc.M601610200 originally published online April 13, 2006
